This article has been published in the Journal of Alloys and Compounds. The final publication is available at Elsevier via https://doi.org/10.1016/j.jallcom.2014.04.140.

Development of a Visco-plastic Constitutive Modeling for Thixoforming of AA6061 in Semi-solid State

JiaoJiao Wang[1, 2], A.B. Phillion[2], GuiMin Lu[1,*]

[1] The Key Laboratory of Pressure Systems and Safety, Ministry of Education, East China University of Science and Technology, Shanghai, 200237, China

[2] Schools of Engineering, University of British Columbia, Kelowna, V1V1V7-BC, Canada

Abstract

A visco-plastic constitutive equation for thixoforming is proposed that takes into account the effect of the liquid fraction along with other factors i.e. strain rate and temperature. The incorporation of liquid fraction allows the model to be applied to any type of semi-solid aluminum alloys a significant improvement over the previous empirical models. Based on the thixotropic compression tests for the semi-solid AA6061 aluminum alloy, this visco-plastic constitutive model is validated by means of simulation on the ABAQUS platform.

Keyword: semi-solid; constitutive modeling; thixoforming; liquid fraction; thixotropic compression.

1 Introduction

A new forming process known as thixoforming has drawn worldwide attention owing to its ability to form spherical-like microstructural morphology during processing, providing the final component with enhanced properties. Thixoforming is a semi-solid processing technique whereby forming occurs in solid-liquid region. Thixoforming processes such as thixotropic die-casting, thixoforging and thixotropic extrusion includes three process segments: semi-solid slurry preparation, re-melting and thixotropic forming. It exhibits less deformation resistance, lower forming temperature, lower energy consumption and cost, and higher performance as compared

* Correspondence author: GuiMin Lu, Tel: +86-21-64252065, Fax: +86-21 64252501, gmlu2013@gmail.com

to conventional casting and forging[1]. Most commonly, thixoforming is applied to aluminum alloys components for the automotive industry. The wrought aluminum alloy AA 6061, the research objective of this paper, has reasonable mechanical properties and thixoformability, enabling the formation of parts such as wheels and steering knuckles[2]. However, as thixoforming is completed in only a few seconds, it is difficult to experimentally investigate some properties, such as the spatial distribution of the solid, the mechanisms of microstructure evolution, and semi-solid constitutive behavior. Instead, constitutive modeling and numerical software tools have been used to precisely predict the deformation behavior for thixoforming. Modelling of constitutive relationship for semi-solid alloys is a key foundation for the theoretical study and further finite element analyses.

A number of constitutive equations have been proposed to describe the behavior of semi-solid alloys in the past decades. Power law model[3] is used to analyze the shear-thickening or thinning behaviors in the semi-solid alloys. The initial deformation behavior of semi-solid alloys can be captured by Bingham model[4]. The Herschel-Bulkley fluid model[5] is applied to describe the behavior of yield region. The creeping flow behavior of semi-solid slurry can be described by Carreau model[6]. In the micro-macro model[7], the deformation is assumed as macroscopically homogeneous and both solid and liquid is regarded as isotropic and incompressible. The semi-solid microstructure is composed of ‘inclusion’ and ‘active zone (coating)’. This model mainly focuses on the elastic-viscoplastic response but ignores the hardening and the real shape of semi-solid microstructures. Burgos, Alexandrou and Entov[8] presented a point view that the transient behavior of shear thickening happens at a constant semi-solid structure, and there exists a yield stress which is resulted from the continuous solid skeleton. The effective volume fraction (EVF)[9] can be calculated the real solid fraction, which ignores the effect of entrapped liquid. However, whether or not the liquid entrapped inside the solid agglomerates participates in the deformation is still a dispute.

So far the properties of thixoforming are not completely explored and there remains disparities in quantitative literature with respect to shear thinning or thickening[10], thixotropic recovery[11], yield stress[12], and the presence or absence of a plastic threshold[13]. The constitutive laws for semi-solid alloys presented in literature can only describe part of the semi-solid deformation behavior. Most of research work concentrated on the strain softening stage[14] or microstructural

evolution process [15]. At present there is no constitutive law that can be applied to comprehensively capture the behavior of thixoforming at different deformation stages. The semi-solid behavior was expressed by means of a single modulus, viscosity, even in the micro-macro model [7]. Therefore, more efforts are needed to achieve a consensus in the choice of a constitutive relationship for thixoforming by theoretical and experimental research.

In the present work, compression tests were conducted on thixoformed AA6061 specimens at different temperatures within the semi-solid region and at different strain rates to determine semi-solid behavior of this unique microstructure. Three types of behavior at different stages of stress/strain curves during thixoforming for semi-solid alloys were investigated. Based on the experimental results, a new constitutive law was tuned and then validated using the ABAQUS finite element software.

2 Experiment

2.1 Semi-solid microstructures

The material investigated was an AA6061 aluminum alloy, with a chemical composition as given in Table 1. Compared with dentritic structure produced by traditional casting (as shown in Fig.1 (a)), the main features of the thixoforming structure is the co-existence of two phases (solid and liquid) and grain spheroidization, as shown in Fig.1 (b). The priority of this globular microstructure enables reduced deformation force and high-quality products.

Liquid fraction for semi-solid alloys has a great influence on the microstructures during thixoforming due to the deformation occurred at a temperature between the solidus and the liquidus. For the calculation of liquid fraction, Lever Rule is usually used for equilibrium solidification while the Scheil equation is for non-equilibrium processes. However, for industrial alloys, such as AA6061, it is hard to determine and verify the value of the partition coefficients for the Scheil equation through experimentation and consequently very few reliable value have been published in existing literature. In Lashkari te.al research work [16], it was proved that either the Lever Rule or the Scheil equation work well to calculate the liquid fractions for these alloys, both calculations are approximately the same at semi-solid temperature ranges.

In addition, the temperature filed was assumed to be homogenous in this work and it viewed as an equilibrium process during deformation. Therefore, the given values of solid fraction f_S are based on the temperature form of the Lever Rule as shown below,

$$f_s = \frac{T_L - T}{T_L - T_s} \tag{1}$$

Where T_S and T_L denote the solidus and liquidus temperature (K) respectively, and T is the test temperature (K).

According to equation (1), the liquid fractions at the test temperatures of 858, 868, and 878 K were about 0.04, 0.18 and 0.32, respectively, and thus a variation in solid fraction is achieved by testing specimens at different temperatures. The semi-solid microstructures at three different solid fractions were investigated before thixotropic compression tests, as shown in Fig.2.

AA6061 belongs to $Al\text{-}Mg\text{-}Si$ alloys, the first ternary eutectic temperature is 858 K and the composition is $\alpha\text{-}Al$, $\beta\text{-}AlFeSi$, Mg_2Si [17]. When deformation temperature was 858 K, i.e. liquid fraction was 4%, ternary eutectic structure started to melt and thus some liquid appeared at grain boundary in the metallographic structure after quenching, as shown in Fig.2 (a). With the temperature increasing, binary eutectic contained $\alpha\text{-}Al$, $\beta\text{-}AlFeSi$ and the second ternary eutectic structure included $\alpha\text{-}Al$, $\beta\text{-}AlFeSi$, Si began to transform into liquid [17-18], so more liquid presented in the semi-solid microstructures, as shown in Fig.2 (b) and (c).

2.2 Thixotropic compression tests

The semi-solid temperature range of AA6061 aluminum alloy is 855-925 K [19]. The experimental procedure is described below. First, the material was processed via near-liquid semi-continuous casting[20] in order to create blanks with microstructure representative of the thixoforming process. Second, small cylindrical compression samples with dimensions Φ8×15 mm were fabricated. Third, thixotropic compression tests at different temperatures and strain rages were carried out by using a Gleeble 3800 thermal-mechanical simulator in order to

measure the stress/strain behavior.

During semi-solid compression tests, two shallow grooves filled with lubricant were made in both sides of the specimen to reduce the friction between clamps and the sample, and then samples were reheated to the semi-solid region by means of the electrical resistance method. The reheating rate was controlled by magnitude of electric current in Gleeble system and two stages of reheating rates were applied during reheating process. The variation of temperatures was recorded by a thermocouple, which was located in the middle section of the specimen. The time-temperature profile during the compression testing is shown in Fig.3, while the experimental matrix (temperatures, strain rates, maximal strain) is given in Table 2. A water quench was carried out immediately afterwards in order to preserve the deformation microstructures and the entrapped liquid.

The reason for two stages of reheating are that the temperature distribution was not ideally homogenous within the specimen. In order to ensure a uniform temperature field during compression tests, the heating rate was decreased from $5\,K\cdot s^{-1}$ to $1\,K\cdot s^{-1}$ when heating temperature was close to the solidus, and then the sample was hold isothermally for 10 s at the target deformation temperature, as shown in Fig.3. Furthermore, uniform temperature zone nearby the thermal couple were considered to be mainly of research interest. Therefore, the temperature within the specimen was regarded as uniform in present work.

2.3 Results

2.3.1 Stress/strain curves of thixoforming

The curves of nominal stress/strain obtained from the compression tests are shown in Figs. 4 and 5. The constitutive behavior for thixoformed AA6061 in the semi-solid state is described by these two figures. Fig. 4 provides the nominal stress/nominal strain behavior at a temperature of 858 K (f_S~0.96) at different strain rates, while Fig. 5 shows the effect of solid fraction on nominal stress/strain at a strain rate of 0.01 s^{-1}.

The results are as expected since stress increases with increasing strain rate for a constant deformation temperature but decreases with increasing fraction solid for a constant strain rate.

The value of strain corresponding the peak stress is found to be around 0.06. The stress/strain curves of thixotropic compression can be divided into three stages. (1) Strain hardening, in which the flow stress increased rapidly and reached a peak value as deformation is applied from a strain of 0 to 0.06. At this deformation stage, strain hardening played a dominant role rather than the dynamic recrystallization. Grain rearrangement appeared within semi-solid microstructures and local deformation happened in grain boundaries with effective lubrication action of the liquid during semi-solid two-phase interval. The sliding and rotation of the solid agglomerates finally resulted in the global deformation of solid skeleton, and thus the stress was dramatically increased[21]. (2) Thixotropic strain softening, in which the stress decreased upon further increase in strain. The sudden decrease in stress can be attributed to the breakdown of the solid skeleton and dynamic recrystallization. (3) Steady-state deformation, in which strain hardening and dynamic recrystallization reached a dynamic balance. In this deformation stage, strain hardening and dynamic recrystallization took effect simultaneously within the semi-solid microstructures. Their role in deformation: a common phenomenon in which continued strain hardening increased the strength of semi-solid specimen, whereas dynamic recrystallization was responsible for softening mechanism to the semi-solid structures. Interactions between strain hardening and dynamic recrystallization could be counterbalanced to a certain extent.

The result of these experiments showed that the change in stress was very slight with strain in the last deformation stage. The compression stress/strain curve presented as a steady horizontal line or existed some small fluctuation in the third steady-state deformation stage, as shown in Figs. 4 and 5. This was due to the different contributions of strain hardening and dynamic recrystallization in semi-solid structures, it was a dynamic process and could approximately cancel each other out.

The maximal peak in stress during these tests was approx. 20 MPa , at f_S=0.96 and a strain rate of 1 s^{-1}, while the minimum stress peak was 2 MPa at f_S=0.68 and a strain rate of 0.01 s^{-1}. Recent work by Xiaolu's[22] and Kim's[23] has also shown that the max peak stresses during thixoforming, at about 8 and 4 MPa respectively, are always quite low owing to the fact that thixoforming occurs in the two-phase regime. The low peak stresses and large ductility found during thixoforming provide a significant advantage over traditional forming processes since this reduces the amount of force required for deformation.

3 Theory

3.1 Empirical constitutive relationship

During thixoforming, the constitutive behavior is a function of the strain, strain rate and temperature, as shown in Figs. 4 and 5. Using these observations, a constitutive law can be derived that includes the following:

(1) when the temperature and strain rate are constant, the relationship between the stress and strain can be written as

$$\sigma = k_1 \varepsilon^n \tag{2}$$

Where σ is stress, ε is strain, n is strain hardening index and k_1 is a constant related to strain.

(2) when the temperature and strain are constant, the relationship between the stress and strain rate can be written as

$$\sigma = k_2 \dot{\varepsilon}^m \tag{3}$$

Where $\dot{\varepsilon}$ is strain rate, m is strain rate sensitivity and k_2 is a constant related to strain rate.

(3) when the strain and strain rate are constant, the relationship between the stress and temperature can be written as

$$\sigma = k_3 e^{-bT} \tag{4}$$

Where T is temperature, b is the temperature coefficient and k_3 is a constant related to temperature.

Based on the above relations, an empirical constitutive relationship can be proposed as follows,

$$\sigma = e^{a-bT} \varepsilon^n \dot{\varepsilon}^m \tag{5}$$

Where *a* is a material constant and its value equal to $\ln k_1 k_2 k_3$.

Equation (5) is similar to the well-known Ludwik equation[24] for modeling constitutive behavior with strain and strain-rate sensitivity. After extracting the experimental data $(\sigma, \varepsilon, \dot{\varepsilon}, T)$ from the compression tests, the material constants in equation (5) can be determined for AA6061 in the semi-solid state by multiple linear regression analysis as shown in Table 3. The experimental data shown in Figs. 4 and 5 was converted from nominal stress/strain to true stress/strain. The volume of the sample calculated from the initial size (Φ8×15) was assumed to be constant during compression, and also that there was no barreling during deformation.

In contrast to the Ludwik equation where strain hardening is achieved owing to *n* being a positive number, the strain softening observed in Figs. 4 and 5 is achieved from a negative value of *n*. Please note that a negative '*n*' means '1/ *n*'.

3.2 Empirical constitutive law verification

In order to test the validity of the empirical constitutive relationship, equation (6), with the parameters given in Table 3, a small finite element model simulating the compression test conditions was developed within the commercial FE software: ABAQUS. The simulation was axi-symmetric and consisting of 4-noded elements. The isotropic elastic modulus and isotropic Poisson's ratio were assumed to be 10 GPa and 0.30[25-26] respectively.

Although Young's modulus depends on temperature, the value is not expected to change significantly over the range of temperatures appeared during the compression tests (858-868*K*).Consequently, it was assumed to remain constant.

The elastic and viscoplastic mechanical properties of semi-solid AA6061 alloys were investigated separately in finite element software ABAQUS to fully take three stages of the stress/strain behavior into account for semi-solid alloys. First, elastic modulus, Poisson's ratio as the input constitutive behavior required for the elastic analysis, and then the UHARD subroutine was utilized to implement equation (6) within the ABAQUS framework with the addition of the parameters ε_0 and $\dot{\varepsilon}_0$ for numerical stability, as shown below,

$$\sigma = e^{(64.23985-0.07363T)}\left(\varepsilon+\varepsilon_0\right)^{-0.7437}\left(\dot{\varepsilon}+\dot{\varepsilon}_0\right)^{0.20555} \quad (6)$$

Where ε_0 is given the value 0.05 and $\dot{\varepsilon}_0$ is given the value $1e^{-5}$ in order to ensure that plastic deformation does not occur until a reasonable stress is achieved for yielding to occur.

The results of this initial verification are shown in Fig.6. The simulation was carried out at temperature of 878 K and strain rate of $0.01s^{-1}$. It was assumed that there was no more change in the liquid fraction during testing at constant temperature. As can be seen, the results were found to be roughly consistent with the experimental data after the peak strain and hence it can be concluded that there are some limitations to applying this empirical equation to a semi-solid analysis. Equation (5) is usually applied to simulate the empirical constitutive relationship of traditional forging or fully solid deformation, in which the deformation temperature is below the solidus. For thixotropic compression, the solid fraction, liquid fraction, phase distribution, and porosity can all cause additional deviations. The main challenge in using equation (5) is that although the regression analysis produced data points with a good multiple correlation coefficient as shown in Table 3, the properties are changing rapidly as a function of temperature, as a result of the changing fraction liquid, and so there is not enough variability in the parameters *a* and *b* to capture the effect of the exiting entrapped liquid during compression. These two parameters are not sensitive enough to capture liquid fraction effect, the reason is that the exponential is too sensitive to changes in *b*, whereas introducing an adjustment factor β allows for small changes to be modelled to take the effect of liquid fraction into consideration.

As shown in the Figs.6, 7, 8, 9, the effect of elastic was studied by the ABAQUS software according to the input value of elastic modulus and Poisson's ratio, the elastic behavior at initial increasing stage on the stress/strain curves was coherent with the experimental data, discrepancy only appeared after peak stress value. ABAQUS took care of the transition between elastic and viscoplastic regime. The viscoplastic behavior after peak stress was our main of point.

3.3 An improved visco-plastic constitutive model for thixoforming

The influence of liquid fraction was not considered in the constitutive law outlined above. From

the compression tests on thixoformed material, it is known that the flow stress is associated with temperature, strain and strain rate. However, when aluminum alloys deform above the solidus temperature, the liquid fraction will also greatly affect the magnitude of stress, as shown in Fig.6. For semi-solid tensile deformation, other authors have modified classical constitutive laws to take into account the deleterious effects of the liquid. Drezet and Eggeler modified a creep law to describe semi-solid tensile behaviour by assuming that the liquid cannot carry any load but instead it is carried entirely by the existing solid network[27]. Van Haaften et al.[28] considered that the critical term for semi-solid tensile behavior was not the liquid fraction, but the fraction of grain boundary covered by the liquid phase. Based on this previous work for simulating tensile deformation in semi-solid material, it is proposed to incorporate the liquid into a constitutive law for thixoforming by including an adjustment factor as shown below,

$$\sigma = e^{(a-bT)}\left(\varepsilon+\varepsilon_0\right)^n\left(\dot{\varepsilon}+\dot{\varepsilon}_0\right)^m\left(1-\beta f_L\right) \tag{7}$$

Where f_L is the liquid fraction of semi-solid alloys given as (1-f_S), and β is a material constant related to the liquid fraction.

In order to tune the value of β, a series of simulations were run in ABAQUS with β set at different values between 0.9 and 1.5 as shown in Fig.7. The simulation was carried out at a temperature of 878 K and strain rate of 0.01s^{-1}, i.e. the same conditions as used previously in Section 3.2 to demonstrate that equation(5) is not sufficient as a constitutive law for semi-solid deformation during thixoforming. For the same parameters as shown in Table 3, the optimal value of β was found to be 1.2.

4 Validation

4.1 Theoretical and experimental comparison

The accuracy of this improved thermal-visco-plastic constitutive equation for characterizing material during thixoforming was established by comparing the numerical and experimental results as shown in Figs. 8 and 9. The range of deformation temperature (fraction solid) used was 858 (f_S=0.96) to 878K (f_S=0.68). The strain rates were from 0.01 to 1 s^{-1}.

As shown in Figs. 4 and 8 the stress decreased as the strain rate was decreased for a given deformation temperature. As expected, the flow stress was sensitive to the strain rate. The value of strain rate decided the speed and degree of load required during the compression. At lower strain rates, the deformation resistance could be reduced because there was sufficient time for liquid phase to flow. At higher strain rates, the compression deformation can be completed in a short time, but the liquid could not participate in deformation. The primary mechanisms of deformation were then solid-phase plastic deformation and grain boundary sliding between the solid particles [21]. This resulted in a higher deformation resistance at high strain rates, which industrially would increase processing costs. However, aluminum alloys that are thixoformed at higher strain rate will contain better thixotropic properties, which is beneficial for the industrial applications of thixoformed parts.

Thixotropic properties means that the viscosity of semi-solid alloys decrease with increasing strain rate, the semi-solid slug may be handle-able like a solid at rest but also exhibit as a liquid-like behavior under the action of applied strain rate, i.e. thixotropic behavior depends on time and strain rate. The viscosity is relatively low especially at high strain rate, the semi-solid material is easy to deform. Therefore, the semi-slid alloy at higher strain rate possess better thixotropic behavior. Specifically, in the range of the strain rate (0.01, 0.1, 1 s^{-1}) studied in present work, the thixotropic behavior at strain rate of 1 s^{-1} was relatively superior to the other two strain rates because its viscosity was thin and resistance to deformation was low. Thixotropy is one of most distinct characteristics for semi-solid alloys during thixoforming, which is very different from conventional casting and forging.

As shown in Figs. 5 and 9, the required flow stress for compressive deformation was reduced as temperature was increased at a given strain rate. Deformation resistance reduced dramatically with the rise in temperature because of the increased amount of liquid. The liquid films located at the grain boundaries of the semisolid become thicker, and with more liquid the morphology of the solid grains became closer to the spherical structures. These spherical-like microstructures facilitate the process of thixoforming. The larger the liquid fraction, the easier for solid particles to slide and rotate (owing to less friction), therefore, less deformation force is needed. The resistance to deformation dropped quickly above a certain critical strain, corresponding to the peak stress, and then a dynamic balance achieved although the strain is increasing. It is found

that dynamic recrystallization occurred during the uniaxial thxiotropic compression for the semi-solid AA6061 alloy.

When the temperature was near the solidus temperature, it is obvious that the small amount of liquid present in the test specimen had little effect on the thixotropic behavior of the semi-solid AA 6061alloy. At higher temperature, the liquid will have considerable effect. In both cases, the constitutive law developed in equation (7) is shown in Figs. 8 and 9 to be valid. The scope of application for this equation are from the deformation temperature (fraction solid) of 858 (f_S=0.96) to 878K (f_S=0.68), and the strain rates from 0.01 to 1 s^{-1}.This range of temperatures and strain rates is well within the norms for thixoforming operations.

Knowledge of a constitutive relation for thixoforming is an important foundation for the theoretical study, technology formulation and die design. Whether (or not) an accurate constitutive relationship for thixoforming can be obtained is a key point of applying finite element simulations to precisely predict the behavior of semi-solid materials. The constitutive equation proposed in this paper can comprehensively describe the thixotropic behavior of semi-solid AA 6061 aluminum alloys. This improved law also extends the material database of the finite element software and establishes the simulation framework for thixotropic constitutive behavior of semi-solid aluminum alloys deformed above the solid temperature. It can be applied to simulate and optimize the semi-solid microstructure, process parameters and die design.

5 Conclusions

(1) Liquid fraction plays a significant role in the stress induced during deformation of aluminum alloys above the solidus temperature. For a given deformation temperature and liquid fraction, the flow stress is seen to increase with increasing strain rate.

(2) A visco-plastic constitutive relationship that includes the effects of liquid fraction was developed to approximate thixotropic compression tests. The validity of this constitutive relationship was verified by means of simulations on the ABAQUS platform.

This work was supported by the National Natural Science Foundation Project of China (51374109).

6 Tables

Table 1 Chemical Composition of AA6061Aluminum Alloy

	Mg	*Si*	*Cu*	*Mn*	*Fe*	*Cr*	*Zn*	*Ti*	*Al*
6061	1.10	0.80	0.30	0.15	0.40	0.05	0.25	0.15	balance

Table 2 Experimental Parameters of thixo-tropic compression

Alloy	Temperatures (*K*)	Strain rates (s^{-1})	maximal strain
AA6061	858,868,878	0.01,0.1,1	0.6

Table 3 Parameter values in the empirical constitutive equation for AA 6061

a	*n*	*m*	*b*	Multiple correlation coefficient
64.23985	-0.7437	0.20555	-0.07363	0.95463

7 Figures

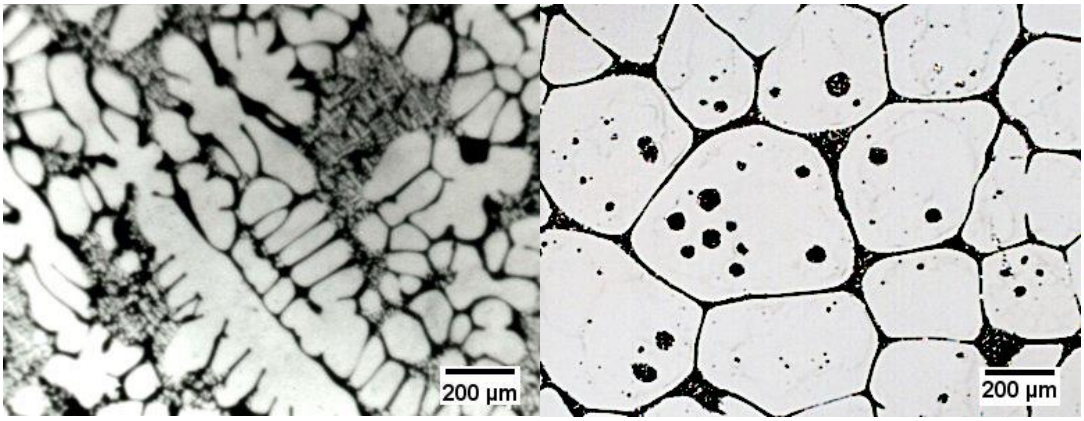

(a) (b)

Fig.1 Variation of microstructures for aluminum alloy at different forming process: (a) Dendritic microstructure of traditional casting, (b) Globular microstructure of thixoforming

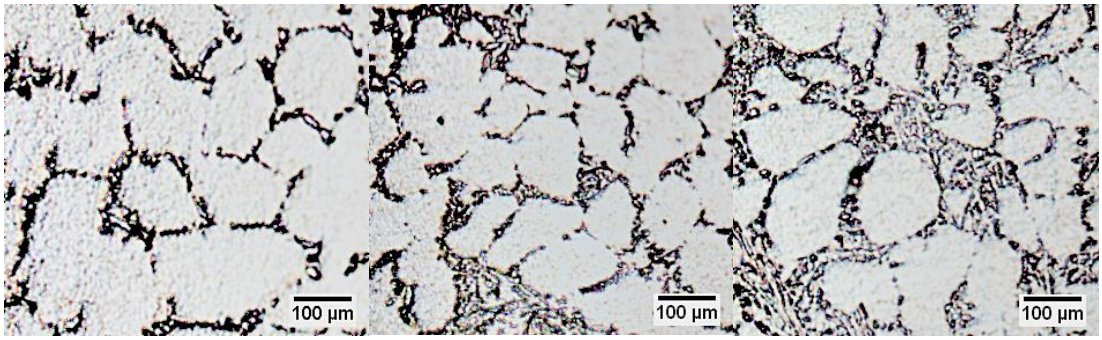

(a) (b) (c)

Fig.2 Semi-solid microstructures at three different solid fractions (a) 0.96 (b) 0.82(c) 0.68 for AA6061 aluminum alloy before thixotropic compression tests.

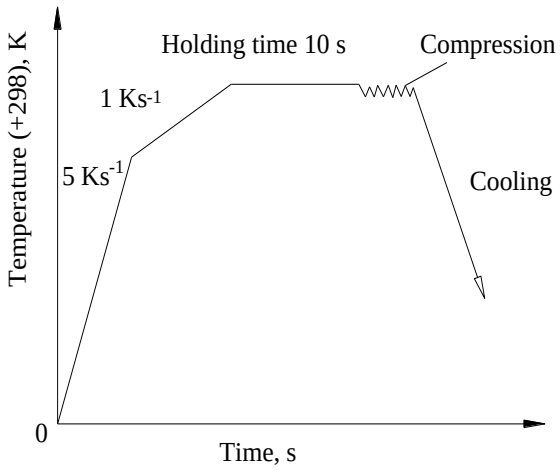

Fig.3 Experimental scheme of thixotropic compression tests

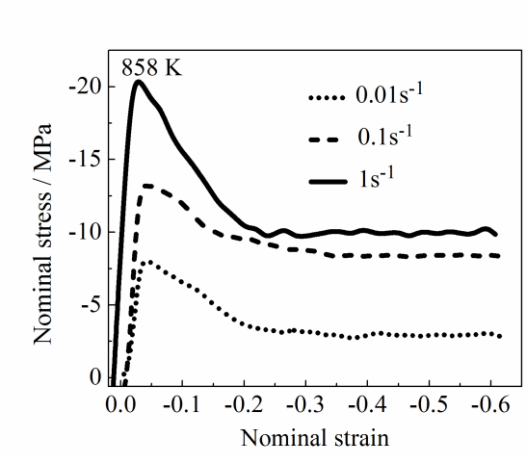

Fig.4 Effect of strain rate on the nominal stress-strain behavior of thixo-cast 6061 aluminum alloy during semi-solid compression testing at 858K (f_s~0.96)

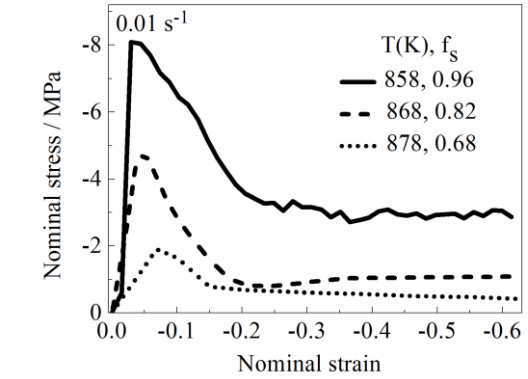

Fig.5 Effect of temperature on the nominal stress-strain behavior of thixo-cast 6061 aluminum alloy during semi-solid compression testing at a strain rate of 0.01 s^{-1}

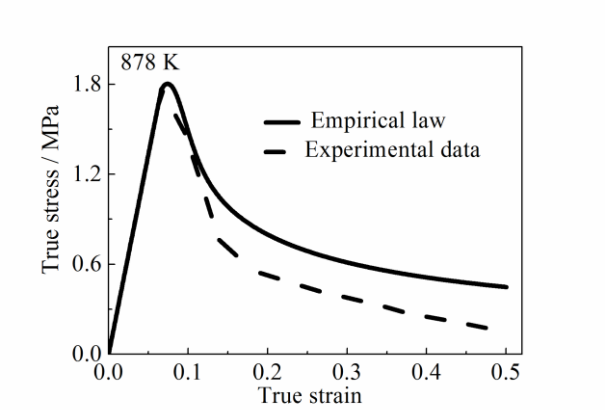

Fig.6 Validation of empirical law against experimental data, results taken at 878 *K* (f_s~0.68) and a strain rate of 0.01 s^{-1}

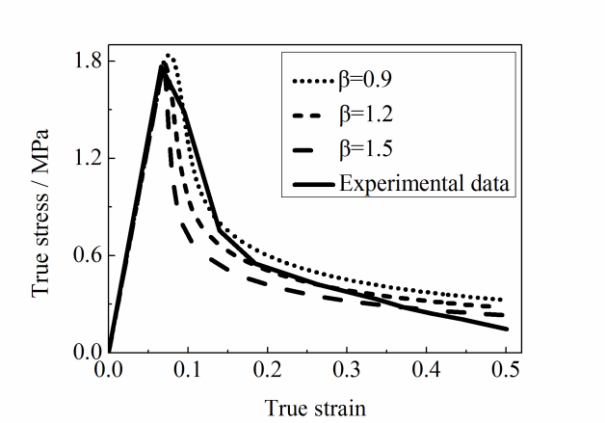

Fig.7 Material parameter determination in the improved constitutive relationship by comparing the simulation results and experimental data obtained at 878 K (f_s~0.68) and a strain rate of 0.01s^{-1}.

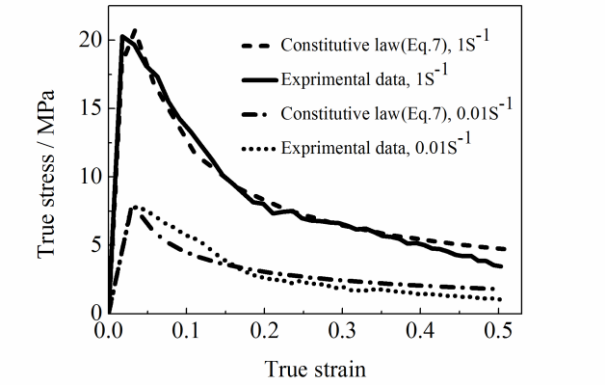

Fig.8 Validation of the constitutive relationship for semi-solid thixo-cast AA6061 alloy against the experimental data obtained at 858K (f_s~0.96*)* and a strain rate of 0.01s^{-1}, 1s^{-1}.

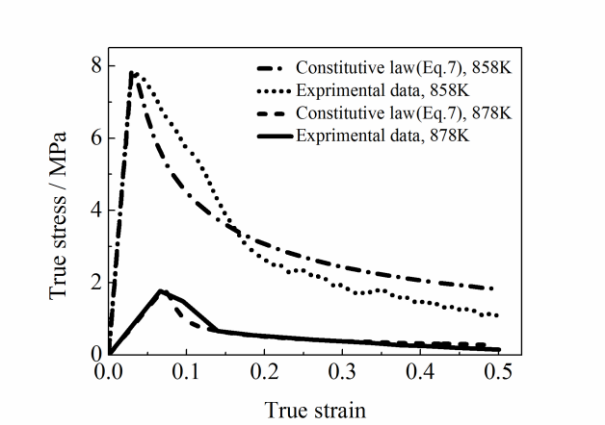

Fig.9 Validation of the constitutive relationship for semi-solid thixo-cast AA6061 against the experimental data obtained at at a strain rate of 0.01 s^{-1} and temperatures of 858 K (f_s~0.96), 878 K (f_s~0.68)

8 Reference

[1] R. Kumar, N. Kumar Singh, R. Ohdar, Optimization of the Process Parameters of Semi-solid Forging of A356 Aluminum Alloy, Int. J. Eng. Sci. Tech. 4(2012) 889-896.

[2] S.Y. Lee, S.I. Oh, Thixoforming characteristics of thermo-mechanically treated AA 6061 alloy for suspension parts of electric vehicles, J. Mater. Process. Tech. 130-131(2002) 587-593.

[3] F. Pineau, G. D. Amours, Prediction of shear-related defect locations in semi-solid casting using numerical flow models, T. Nonferr. Metal. Soc. 20(2010) 878-882.

[4] S. Z. Shang, J. J. Wang, G. M. Lu, W. N. Zhang, X. L. Tang, Numerical Simulation of Thixo-diecasting Al6061 Alloy Automobile Part, Adv. Mater. Res. 418-420(2012) 1456-1459.

[5] S. Simlandi, N. Barman, H. Chattopadhyay, Study on Rheological Behavior of Semisolid A356 Alloy during Solidification, Trans. Indian. Inst. Met. 65(2012) 809-814.

[6] G. L. Zhu, J. Xu, Z. F. Zhang, G. J. Liu, Numerical simulation of die filling behavior of AZ91D in the semisolid process, Res. Dev. 7(2010) 127-131.

[7] V. Favier, H. V. Atkinson, Micromechanical modelling of the elastic–viscoplastic response of metallic alloys under rapid compression in the semi-solid state, Acta Mater. 59(2011) 1271-1280.

[8] G. R. Burgos, A. N. Alexandrou, V. Entov, Thixotropic rheology of semisolid metal suspensions, J. Mater. Process. Tech. 110(2001) 164-176.

[9] M. Perez, J.C. Barbe, Z. Neda, Y. Brechet, L. Salvo,Computer simulation of the microstructure and rheology of semi-solid alloys under shear, Acta mater. 48 (2000) 3773-3782.

[10] M. Modigell, A. Pola, Modeling of shear induced coarsening effects in semi-solid alloys, T. Nonferr. Metal Soc. 20(2010) 1696-1701.

[11] H. Shimahara, R. Baadjou, R. Kopp, G. Hirt, Investigation of flow behaviour and microstructure on X210CrW12 steel in semi-solid state, Solid State Phenom. 116-117(2006) 189-192.

[12] J. Koke, M. Modigell, Flow behaviour of semi-solid metal alloys, J. Non-Newton. Fluid Mech. 112(2003) 141-160.

[13] V. Favier, H. V. Atkinson, Analysis of semi-solid response under rapid compression tests using multi-scale modelling and experiments, T. Nonferr. Metal Soc. 20(2010) 1691-1695.

[14] B. Liu, X.G. Yuan, H. J. Huang, S. H. Zhang, Semi-Solid Deformation of Al-Fe Alloy Prepared by Electromagnetic Stirring, Adv. Mater. Res. 152-153(2010) 726-733.

[15] S. B. Hassas-Irani, A. Zarei-Hanzaki, B. Bazaz, Ali A. Roostaei, Microstructure evolution and semi-solid deformation behavior of an A356 aluminum alloy processed by strain induced melt activated method, Mater. Des. 46(2013) 579-587.

[16] O. Lashkari, S. Nafisi, J. Langlais, R. Ghomashchi, The effect of partial decanting on the chemical composition of semi-solid hypo-eutectic Al–Si alloys during solidification, J. Mater. Process. Tech. 182(2007) 95-100.

[17] S. N. Samaras, G. N. Haidemenopoulos, Modelling of micro-segregation and homogenization of 6061 extrudable Al alloy, J. Mater. Process. Tech. 194(2007) 63-73.

[18] G. Sha, K. O'Reilly, B. Cantor, J. Worth, R. Hamerton, Growth related metastable phase selection in a 6xxx series wrought Al alloy, Mater. Sci. Eng. A 304-306(2001) 612-616.

[19] D. Maisonnette, M. Suery, D. Nelias, P. Chaudet, T. Epicier, Effects of heat treatments on the microstructure and mechanical properties of a 6061 aluminium alloy, Mater. Sci. Eng. 528(2011) 2718-2724.

[20] S. Z. Shang, J. J. Wang, G. M. Lu, X. L. Tang, Study on the Semi-Solid Thixo-Diecasting Process of Aluminum Alloys and Die Design, Solid State Phenom. 192-193(2012) 460-465.

[21] S. S. Xie, X.G. Li, Y. X. Jiang, Rigid-Viscoplastic finite element analysis on semi-solid thixoforming automobile wheel of AZ91D magnesium alloy, J. plasticity Eng. 12(2005) 89-93.

[22] X. L. Yu, F. G. Li, M.Q. Li, Modelling and optimization of general constitutive equation of semi-solid thixoforming, Chin. J. Mech. Eng. 43(2007) 72-76.

[23] W. Y. Kim, C. G. Kang, B. M. Kim, The effect of the solid fraction on rheological behavior of wrought aluminum alloys in incremental compression experiments with a closed die, Mater. Sci. Eng. A 447(2007) 1-10.

[24] A. K. Maheshwari, A Computational Method to crosscheck & consistently Unifying the Deformation Test Experimental Results, Int. J. Comput. Sci. Emerg. Trends 01(2012) 18-25.

[25] M. Sistaninia, A.B. Phillion, J. M. Drezet, M. Rappaz, Simulation of semi-solid material mechanical behavior using a combined discrete/finite element method, Metall. Mater. Trans. 42(2011) 239-248.

[26] O. Ludwig, J. M. Drezet, C. Martin, M. Sury, Rheological behavior of Al-Cu alloys during solidification: Constitutive modeling, experimental identification, and numerical study, Metall. Mater. Trans. A.36 (2005) 1525-1535.

[27] J. M. Drezet, G. Eggeler, High apparent creep activation-energies in mushy zone microstructures, Scrip. Metall. Mater. 31(1994) 757-762.

[28] W. V. Haaften, B. Magnin, W. Kool, L. Katgerman, Constitutive behavior of as-cast AA1050, AA3104, and AA5182, Metall. Mater. Trans. A 33(2002) 1971-1980.